

Biomedical Physics & Engineering Express



PAPER

Dosimetric parameters calculation for 18 MV photon beam in flattening filter (FF) and flattening filter free (FFF) linear accelerators with and without magnetic deflector and lead filter

RECEIVED
3 October 2023

REVISED
12 January 2024

ACCEPTED FOR PUBLICATION
5 February 2024

PUBLISHED
13 February 2024

Morteza Hashemizadeh¹ , Mansour Zabihzadeh^{1,2,3,*} , Hojatollah Shahbazian³, Jafar Fatahi-Asl⁴ and Marziyeh Reshadatian¹

¹ Department of Medical Physics, School of Medicine, Ahvaz Jundishapur University of Medical Sciences, Ahvaz, Iran

² Cancer Research Center, Ahvaz Jundishapur University of Medical Sciences, Ahvaz, Iran

³ Department of Clinical Oncology, School of Medicine, Golestan Hospital, Ahvaz Jundishapur University of Medical Sciences, Ahvaz, Iran

⁴ Department of Radiologic Technology, Faculty of Paramedicine, Ahvaz Jundishapur University of Medical Sciences, Ahvaz, Iran

* Author to whom any correspondence should be addressed.

E-mail: manzabih@gmail.com

Keywords: dose distribution, electron contamination, flattening filter, lead filter, magnetic deflector (MD), radiotherapy, Monte Carlo (MC) calculation

Abstract

Dosimetric characteristics of the flattening filter (FF) and flattening filter free (FFF) modes of 18 MV therapeutic photon beam were investigated with and without the magnetic deflector (MD) and lead filter. MCNP version 6.1.0 Monte Carlo (MC) code was used to simulate the 18 MV photon beam of 2100 C/D-Varian linear accelerator (LINAC) for the FF and FFF modes. The MD (uniform magnetic flux density of 1 Tesla) and lead filter (thickness of 1 mm) were modeled to remove contaminant electrons. The dosimetric parameters for different scenarios of LINAC's head were calculated. Removing the flattening filter in the FFF mode increased the dose rate, electron contamination, skin dose, out-of-field dose, and un-flatness compared to the FF mode. While the lead filter decreased the contaminant electrons significantly, using the MD removed all secondary electrons from the beam line. The surface dose was decreased by 8.3% and 11.2% for the magnetic deflector (MD) and lead filter in the FF mode, respectively. The surface dose was decreased by 16.8% and 20.3% for the MD and lead filter scenarios in the FFF mode, respectively. The MD and lead filter decreased surface penumbra by 15.5% and 11.5% compared to the FFF mode. Removing the flattening filter from the LINAC's head improves most of the dosimetric characteristics of the 18MV therapeutic beam. The use of a lead filter and magnetic deflector preserves the skin-sparing property of megavoltage beams that deteriorate in FFF mode. However, using a magnetic deflector does not reduce photon fluence and dose rate.

1. Introduction

The presence of charged particles in a therapeutic photon beam may lead to contamination, resulting in a shift of the maximum dose depth towards a shallower depth, an increase in surface dose, and a reduction in skin-sparing effectiveness, which is advantageous in high-energy photon therapy. These charged particles, namely electrons and positrons, are generated through photon interactions within the linear accelerator (LINAC) head components, the air volume between the phantom and the LINAC head. Additionally,

various accessories placed in the beam's path can either decrease or increase the effects on surface doses depending on their material composition and distance from the isocenter. It has been observed that contaminating electrons causes the maximum dose depth to shift towards a shallower depth in the high-energy photon beams [1]. Several authors have reported that the flattening filter (FF) and the beam monitor chamber are the primary sources of electron contamination [2–4]. Moreover, the air volume has also been identified as a significant source, particularly at extended source-surface distances (SSDs) [3].

The FF in the LINAC head ensures the uniform delivery of radiation dose to the target volume at a specific depth in a homogeneous phantom by the bremsstrahlung interaction. Typically, it is placed along the central beam axis and possesses a Gaussian shape depending on the LINAC's energy. The FF commonly comprises high atomic number materials, such as copper (Cu). In modern treatment techniques, which require high-energy photon beams, homogeneous beams are not necessary, as seen in stereotactic body radiation therapy (SBRT), intensity-modulated radiation therapy (IMRT), and LINAC-based radiosurgery [5]. Several studies have reported the concept of free-flattening filter (FFF) beams at various energies [6, 7]. The removal of the FF has been reported to decrease head scatter and increase the dose rate [8, 9], as well as reduce electron and neutron contamination [10, 11], penumbra, and out-of-field doses [6, 12]. The presence of contaminant particles in the FF beam stems from the interaction of bremsstrahlung photons from the x-ray target with electrons and nuclei of the copper, resulting in particle contamination (electrons and neutrons) beyond the FF [10, 11].

It has been suggested that reducing the field size can scatter the contaminating electrons out of the field size, thereby reducing the surface dose [13, 14]. Various studies have employed magnetic fields to eliminate contaminating electrons originating from the LINAC head [15–17]. Some authors have proposed replacing the air volume between collimators and the surface with a helium bag to eliminate electrons produced in the air [18, 19]. Among high-Z filters, a lead filter is the most effective in spreading contaminating electrons and preventing them from reaching the surface [20, 21]. The utilization of modifiers along the path of the radiation beam has the potential to alter the quality of the beam and cause alterations in the dosimetry parameters, particularly within the build-up region [22].

During radiotherapy using megavoltage photon beams, the production of contaminant electrons can cause increased skin and subcutaneous tissue damage due to unwanted dose deposition. Dosimetric aspects of this issue are often reported separately and for different scenarios. Therefore, a comprehensive evaluation of different methods to reduce electron contamination in various techniques can give physicists a complete understanding. In this study the dosimetric properties with a focus on electron contamination were calculated and compared in flattening filter (FF) and flattening filter free (FFF) modes of 18 MV- 2100 C/D Varian LINAC's head using the Monte Carlo (MC) technique; MCNP (Ver. 6.1.0). The magnetic deflector (MD) and lead filter as two techniques for electron contaminant reduction, separately and together, were evaluated in the FF and FFF modes.

2. Method

In this study, the dosimetric characteristics of the 18 MV photon beam focused on electron contamination were investigated for different scenarios of LINAC's head: standard or FF mode (with flattening filter without any tools for removing contaminant electrons), FFF mode (without flattening filter without any tools for removing contaminant electrons), FF mode + MD (magnetic deflector), FFF mode + MD, FF mode + lead filter, FFF mode + lead filter, FF mode + MD + lead filter, and FFF mode + MD + lead filter.

2.1. Experimental measurement

All dose measurements, including depth dose curves and dose profiles of 18 MV-Varian C/D 2100 LINAC for the FF mode, were carried out using a 0.6 c.c. Farmer ionizing chamber (PTW, Freiburg, Germany), the Scanditronix Wellhofer dosimetry system, and OmnoPro software (version 6.4) at $50 \times 50 \times 50 \text{ cm}^3$ IBA blue phantom (IBA dosimetry Schwarzenbruck, Germany). The source-surface-distance (SSD) of 100 cm and field size of $10 \times 10 \text{ cm}^2$ were set to measure the dose data. All dose measurements were performed according to recommendations of the International Atomic Energy Agency (IAEA) protocol, TRS-398 report. Each measurement was repeated three times and its averaged value was reported to ensure the stability of LINAC's output and the maximum error was below 0.5%.

2.2. Monte Carlo calculation

2.2.1. LINAC's head simulation

MCNP version 6.1.0 Monte Carlo code was used to simulate Varian 2100 C/D LINAC with and without the flattening filter (FF and FFF mode, respectively) for the 18 MV photon beam. All LINAC's components, such as electron source, target, primary collimator, vacuum window, flattening filters (only for FF mode), ionizing chamber, mirror, and secondary collimator were simulated precisely by MCNP (Ver. 6.1.0). In the FFF mode, flattening filter was removed and replaced with copper thin foil [23]. The dosimetric data was calculated for SSD of 100 cm and field size of $10 \times 10 \text{ cm}^2$. The electron and photon energy cut-off were 0.5 and 0.01 MeV, respectively. To reach an acceptable relative error about 1% (expect dose profile edges and deeper PDD areas), 1.1×10^9 initial electrons were transported to calculated fluences and absorbed doses. The calculated percent depth dose (PDD) curve and dose profile compared to the measurement data were used to benchmark the LINAC's head model. The gamma index (γ) is one of the most commonly used metrics for dosimetric verification used in this study to evaluate the coincidence between the calculated and measured dose distributions. It provides the metric of the agreement to dose.

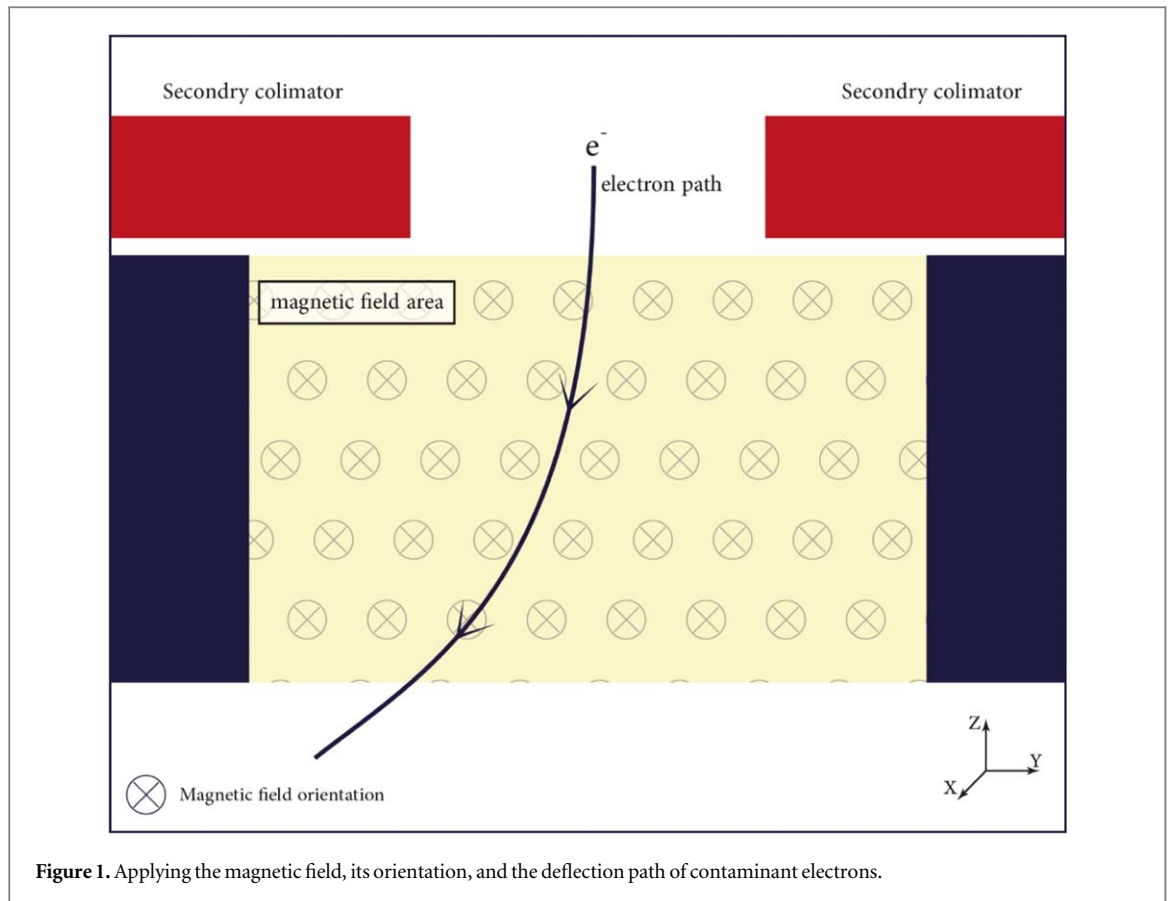


Figure 1. Applying the magnetic field, its orientation, and the deflection path of contaminant electrons.

2.2.2. Lead filter simulation

The electron contamination associated with the 18 MV photon beam affects the measurement dose distribution. However, it can be removed by using a 1 mm lead filter, which reduces unwanted surface dose from contaminant electrons from the accelerator [21, 24]. For both FF and FFF modes, the lead filter thickness was set to 1 mm and was placed immediately below the secondary collimators of LINAC's head and located at 55.4 cm from the surface of the phantom. This filter covers the entire field view of $10 \times 10 \text{ cm}^2$ field size.

2.2.3. Magnetic field simulation for magnetic deflector (MD)

Recently, MCNP 6.1.0 enables the application of a magnetic field in the specified geometry and transporting the particle in it with direct magnetic field tracking using numerical integration techniques [25–28]. More details on the MC transportation of charged particles in the presence of the magnetic field can be found in kinds of literature [29–31]. In this study, the constant magnetic field of 1 T (Tesla) was applied in a $15 \times 15 \times 10 \text{ cm}^3$ space under the secondary collimators of LINAC's head to remove the contaminant electrons from the radiation field. The expected effect of the magnetic field on charged particles (contaminant electrons) is shown in figure 1. The parameters and features for the used constant magnetic field are shown in table 1.

Table 1. Typical parameters for the constant magnetic field used in magnetic deflector (MD).

Magnetic field control card	Keyword	Value
BFLDn	Const	—
	Field	1
	Vec	1 0 0

2.2.4. Dose and fluence calculation

In this study, the voxel dimension was set to $2 \times 2 \times 2 \text{ mm}^3$ to calculate PDD curves and dose profiles in a water phantom ($50 \times 50 \times 50 \text{ cm}^3$). Profile dose was calculated at the surface of the water phantom. The contaminant electron and photon fluences per MeV per initial incident electron on the LINAC target (with an energy bin of 0.01 MeV) were investigated at an air voxel with the dimension of $10 \times 10 \times 0.1 \text{ cm}^3$ in the front surface of the water phantom. The photon and electron cut-off energies were set to 0.01 MeV and 0.5 MeV, respectively. No Rayleigh scattering and other photon interaction forcing were used to keep calculation errors down.

2.3. Result analysis

The dose profile penumbra and un-flatness at the surface of the phantom and dose reduction were calculated for different scenarios by equations of (1), (2), and (3), respectively;

$$\text{Penumbra (mm)} = d_{80} - d_{20} \quad (1)$$

$$\text{Un-flatness (\%)} = \frac{D_{\max} - D_{\min}}{D_{\max} + D_{\min}} \times 100 \quad (2)$$

$$\text{Dose reduction (\%)} = \frac{D_2 - D_1}{D_1} \times 100 \quad (3)$$

Which, d_{80} and d_{20} in penumbra calculation are depth of the 80% and 20% dose profile, respectively. Maximum and minimum dose point values on the profile within 80% of the beam width in the un-flatness dose profile are known as D_{\max} and D_{\min} , respectively. The doses in D_2 and D_1 were compared to determine the dose reduction in different scenarios. The average energy at the surface of the water phantom was determined from the calculated energy spectra by equation (4);

$$\bar{E} = \frac{\sum_0^{E_{\max}} \phi_E E dE}{\sum_0^{E_{\max}} \phi_E dE} \quad (4)$$

Where \bar{E} is average energy, ϕ_E is the photon fluence at energy bin (dE), and E_{\max}

is the maximum energy of the photon. The data resulting from repeated calculations were used to evaluate the uncertainty for each tally quantity X , based on the equation (5);

$$\sigma_X = \sqrt{\frac{\sum_{k=1}^N (X_k - \bar{X})^2}{N(N-1)}} \quad (5)$$

Where N is the number of iterates, X_k is the value of X in iterate k , and \bar{X} is the mean value of X evaluated over all iterates. The maximum relative error of calculation was less than 2%. The Origin 2021 software was used to plot curves and figures. All data for PDD and dose profile curves was normalized to the maximum dose of water phantom on the beam's central axis and in the case of standard mode (LINAC's head with a flattening filter and without any magnetic field or lead filter).

3. Results

3.1. Benchmark the 2100 C/D Varian LINAC's head model

The MC model of the 18 MV photon beam from 2100 C/D Varian LINAC's head was validated against the measurements by gamma index analysis. Using the trial-and-error method, the optimal values for electron energy, spatial FWHM (Full Width at Half Maximum), and mean angular spread were 14.4 MeV, 0.08 cm, and 0.8 degrees, respectively. Implementing these optimal parameters in MC simulations resulted in the calculated data comparable with the measurement data. The measured and MC Calculated data for FF mode are shown in figure 2. The estimated gamma index (<1) with acceptance criteria of 3%/3 mm [32] shows that the measured data and the MC calculated are in good agreement in all points. The maximum

relative dose differences between MC and measurement data were 1.8% and 2.7% in the build-up and semi-equilibrium region, respectively.

3.2. Percentage depth dose curves

The PDD curves on the central beam axis were investigated in the water phantom for $10 \times 10 \text{ cm}^2$ field size at SSD=100 cm. All the PDD curves are shown in figure 3. All curves were normalized to the maximum depth dose of the FF mode. The PDD values in the depth of 10 cm (D_{10}), depth of maximum dose (d_{\max}), and surface dose (D_0) are collected in table 2.

3.2.1. FF mode

The surface dose decreased by 8.3% and 11.2% for the magnetic deflector (MD) and lead filter in FF mode, respectively. The utilization of the MD resulted in a slight reduction in dose within the build-up region compared to the standard case in the FF mode. The MD did not change the maximum dose depth in the FF mode. There is no significant difference between the use of both the lead filter and the MD in PDD compared to the use of only the lead filter.

3.2.2. FFF mode

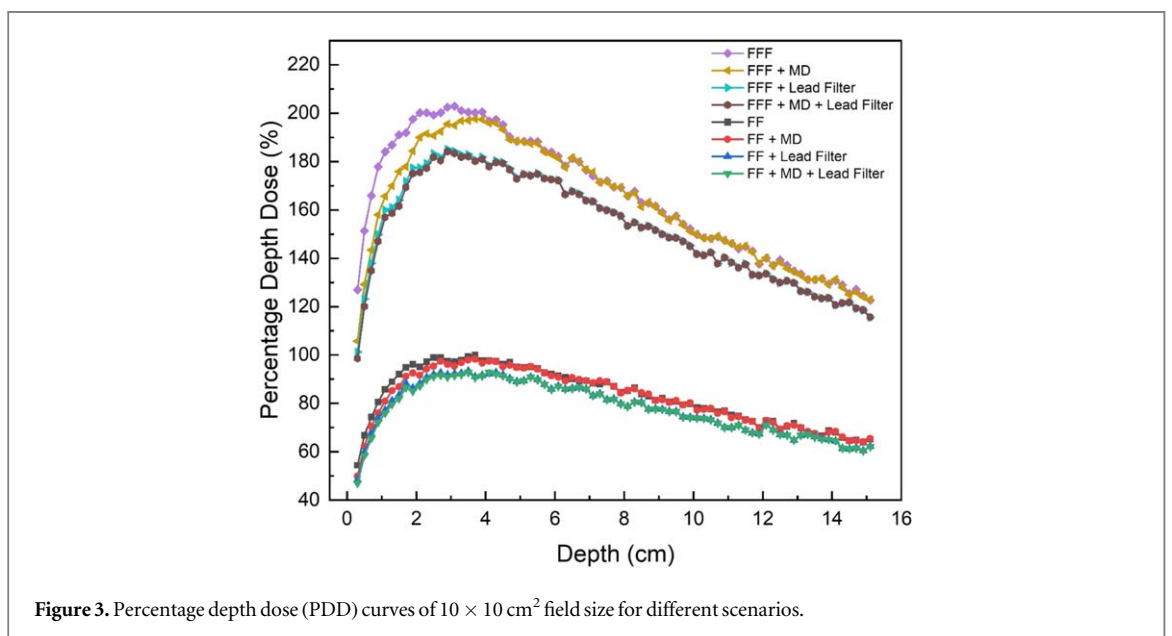
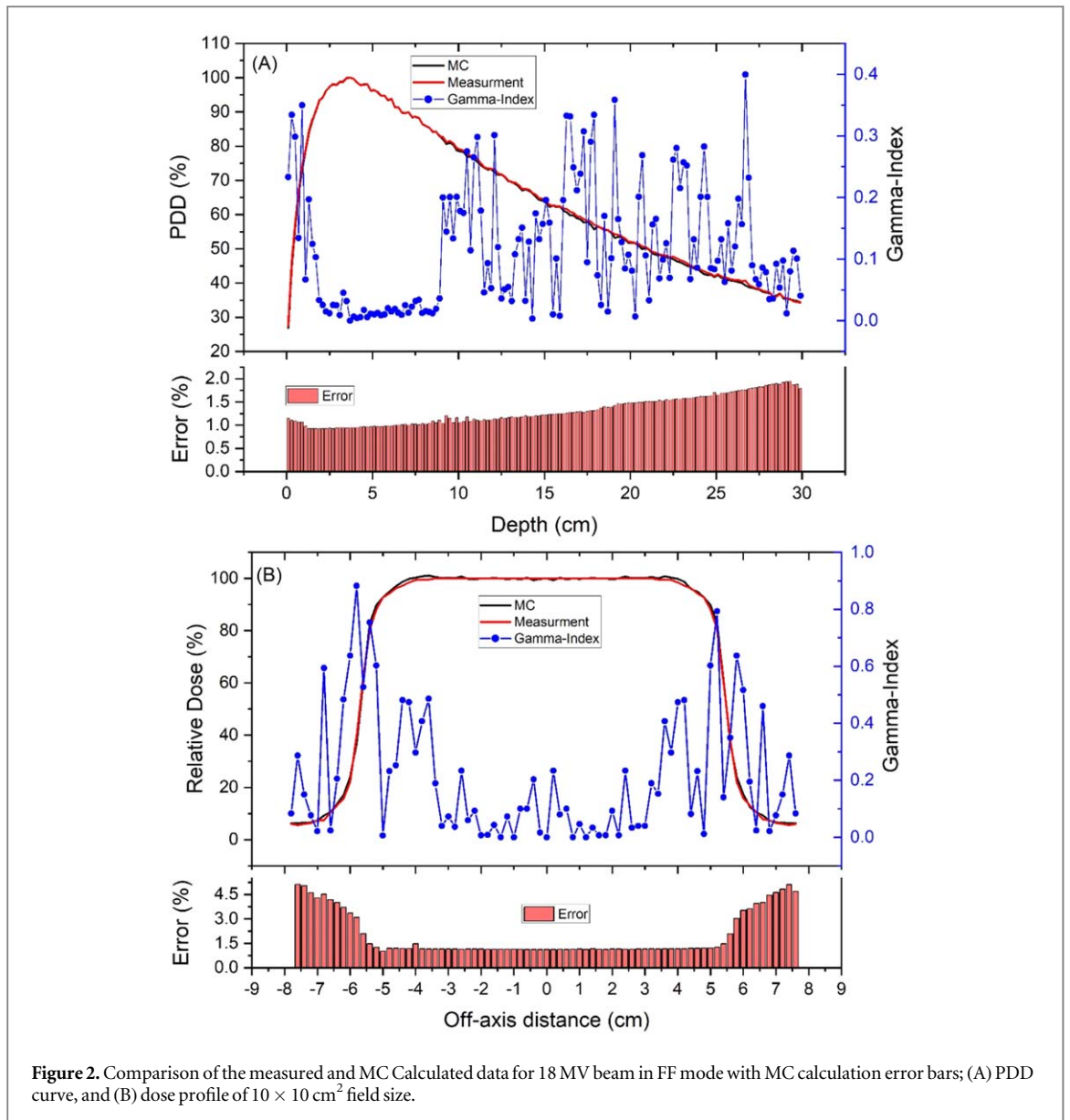
In the FFF mode, the dose was increased compared to the FF mode. Surface dose decreased by 16.8% and 20.3% for the MD and lead filter in FFF mode, respectively. There is no significant difference between the use of both the lead filter and the MD in PDD compared to the use of only the lead filter. The MD and lead filter utilization caused a visible decrease in dose, as shown in figure 3, within the build-up region compared to the FFF mode. Maximum dose depth becomes more profound when the MD is utilized. There is no significant difference in maximum dose depth, whether using both the lead filter and MD or only the lead filter in the FFF mode.

3.3. Relative absorbed dose profiles

The lateral profile dose was calculated at the phantom's surface (depth of 3 mm) with a 2 mm lateral dose resolution. The lateral dose profile is typically measured at a depth of 10 centimeters. However, in this particular study, the primary objective is to investigate and examine the impact of contaminated electrons on the surface of the phantom. Therefore, the lateral profile dose is reported at a shallower depth. The lateral dose profile and its enlarged part at the edge of the field are shown in figure 4.

3.3.1. FF mode

MD and lead filter decreased profile dose penumbra by 6.5% and 3.5% compared to standard FF mode. However, utilizing both MD and lead filter caused the most decreasing profile dose penumbra by 8.28% compared to the standard FF mode. There is no



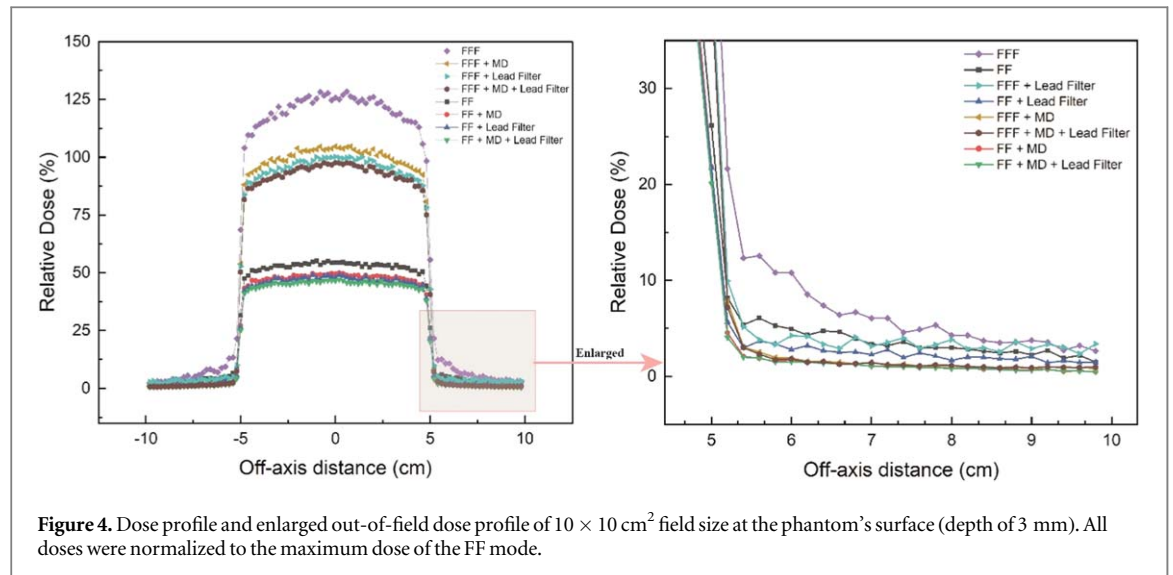


Figure 4. Dose profile and enlarged out-of-field dose profile of $10 \times 10 \text{ cm}^2$ field size at the phantom's surface (depth of 3 mm). All doses were normalized to the maximum dose of the FF mode.

Table 2. PDD at a surface dose (D_0), at a depth of 10 cm (D_{10}), and maximum dose depth (d_{max}) for different scenarios. All doses were normalized to the maximum dose of the FF mode.

Conditions	D_0 (%)		D_{10} (%)		d_{max} (cm)	
	FF	FFF	FF	FFF	FF	FFF
Standard	54.4	127.0	79.8	152.2	3.7	3.1
MD	49.9	105.7	80.2	151.2	3.7	3.7
lead filter	48.3	101.2	74.2	145.2	3.5	2.9
MD + lead filter	46.9	98.6	74.0	145.0	3.5	2.9

significant un-flatness decrease in FF mode, according to table 3. The off-axis dose had undergone many changes, as shown in figure 4. B and table 3. The MD and lead filter decreased the off-axis dose by removing the contaminant electrons. The MD had the most significant impact on off-axis dose reduction. MD and lead filter decreased the off-axis dose at a 6 cm distance by 6.4% and 4.3% compared to standard FF mode. However, utilizing both the MD and lead filter caused the most decrease in the off-axis dose at a 6 cm distance by 6.9% compared to the standard FF mode.

3.3.2. FFF mode

The observed alternations in the dose profile for the FFF mode are more evident than in the FF mode, as shown in figure 4 and table 3. Magnetic deflector and lead filter decreased profile dose penumbra by 15.5% and 11.5% compared to the FFF mode. However, utilizing both MD and lead filters caused the most decreasing profile dose penumbra by 16% compared to the FFF mode. There is a more significant un-flatness decrease in the FFF mode than the FF mode, according to table 3. The MD and lead filter caused decreasing un-flatness compared to the FFF mode by 23.6% and 19%, respectively. However, utilizing both MD and lead filters caused the most decreasing un-flatness by 24.5% compared to the FFF mode. The

Table 3. The Penumbra, Un-flatness, and off-axis doses were calculated from the surface dose profiles in the water phantom for different scenarios.

Conditions	Penumbra (mm)		Un-flatness (%)		Off-axis dose (%) ^a	
	FF	FFF	FF	FFF	FF	FFF
Standard	3.38	3.81	3.33	5.32	4.93	10.78
MD	3.16	3.22	3.15	4.06	1.74	1.90
lead filter	3.26	3.37	3.60	4.31	2.80	4.26
MD + lead filter	3.10	3.20	3.09	4.02	1.52	1.83

^a The off-axis dose at a 6 cm distance.

most off-axis dose belongs to the FFF mode, as shown in figure 4. B and table 3.

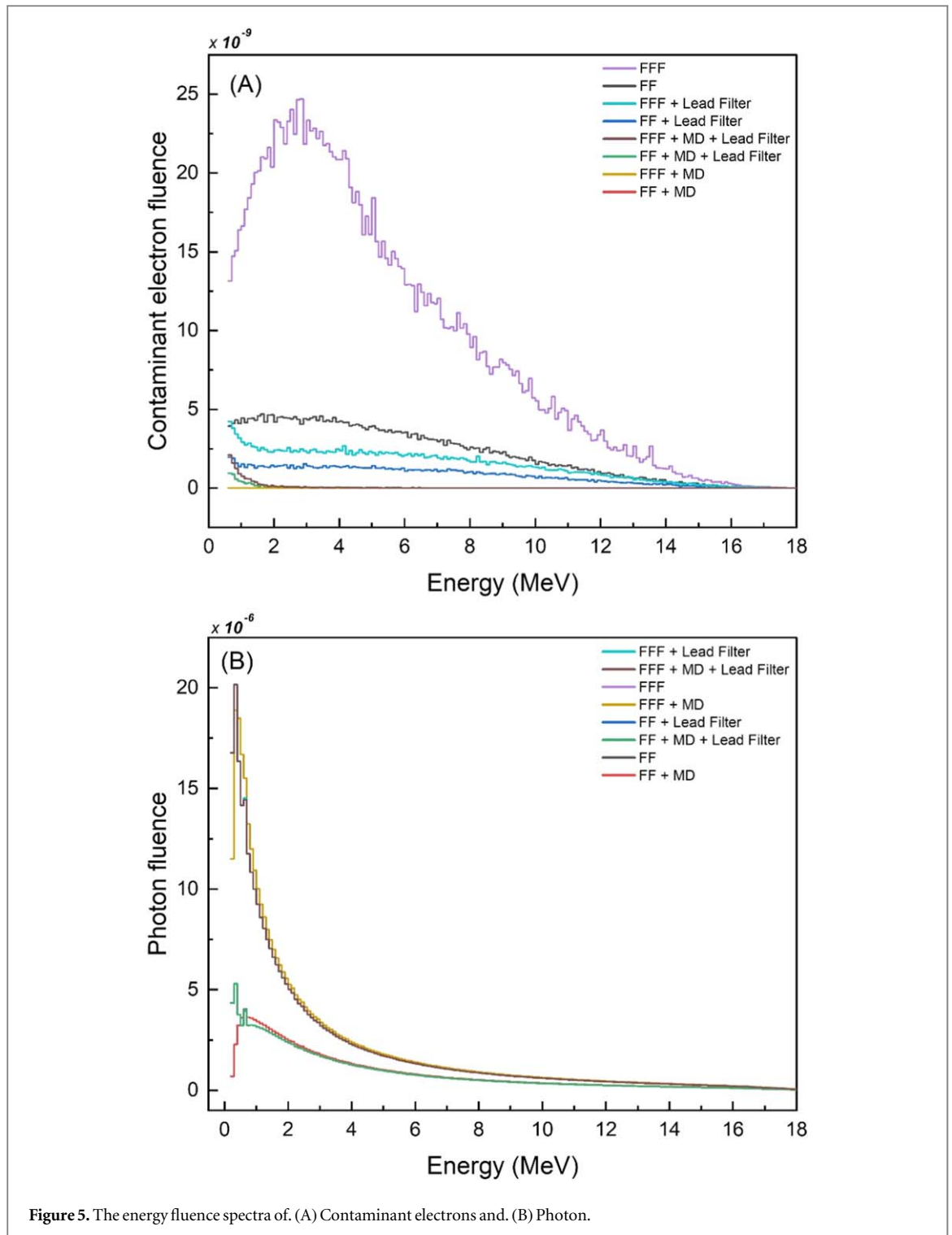
3.4. Photon and contaminant electrons spectra

The photon and the contaminant electron spectra for all scenarios were calculated at SSD of 100 cm (see section 2.2.4) and shown in figure 5. The average energy, the energy of maximum fluence, and the total fluence of the photon and the contaminant electrons at the surface of the phantom are shown in tables 4 and 5, respectively. As expected, removing the flattening filter significantly increases the fluences of photons and contaminant electrons on the surface of the phantom. The increase was three times for photons and five times for contaminant electrons. The MD had a significant impact on reducing electron contamination. However, no significant changes were observed in the photon fluence by using the MD compared to the lead filter.

4. Discussion

4.1. Dose distribution: the FF mode versus the FFF mode

Flattening filters are commonly used in radiotherapy to achieve a uniform dose distribution across the



treatment field. Despite some disadvantages, removing the flattening filter from the LINAC's head (FFF mode) has gained attention due to its potential to improve treatment efficiency [33–35]. Our calculated data for $10 \times 10 \text{ cm}^2$ field size showed that removing the FF increased the total photon fluence; the ratio of photon fluence for the FFF mode to the FF mode was 2.46. Furthermore, from the data in table 2, the dose ratio in reference dosimetry depth of 10 cm for the FFF mode to the FF mode was about 1.91. This increased dose rate can lead to shorter treatment times, as higher

doses can be delivered in a shorter period. From the point of view of clinical application, this increased dose rate has an interesting probability of decreasing the time needed for delivering the prescribed dose to the target volume and decreasing the number of required treatment fractionations using the higher dose at the same time for each fraction [34, 35]. King *et al* (2013) confirmed that this higher dose rate can also improve treatment outcomes by reducing the overall treatment time and minimizing the risk of tumor repopulation during treatment breaks [36]. Kry

Table 4. The Average energy, the energy of maximum fluence, and the total fluence of the photon in different scenarios.

Conditions	Average energy (MeV)		Energy of maximum fluence (MeV)		Total fluence ($\times 10^{-4}$) ^a	
	FF	FFF	FF	FFF	FF	FFF
	Standard	4.19	3.25	0.6	0.3	1.49
MD	4.19	3.25	0.6	0.3	1.49	3.66
lead filter	4.00	3.21	0.3	0.3	1.50	3.56
MD + lead filter	4.02	3.22	0.3	0.3	1.50	3.55

^a The unit of the fluence is the number of photons per cm^2 per particle.

Table 5. The Average energy, the energy of maximum fluence, and the total fluence of the contaminant electrons in different scenarios.

Conditions	Average energy (MeV)		Energy of maximum fluence (MeV)		Total fluence ($\times 10^{-8}$) ^a	
	FF	FFF	FF	FFF	FF	FFF
	Standard	5.5	5.1	1.6	2.8	37.6
MD	0.0	0.0	0.0	0.0	0.0	0.0
lead filter	5.9	5.9	0.6	0.6	13.4	24.2
MD + lead filter	1.4	1.3	0.6	0.6	0.6	1.1

^a The unit of the fluence is the number of electrons per cm^2 per particle.

et al (2007) reported that neutron fluence per monitor unit of 18 MV beam was approximately 20% lower in the FFF mode than in the FF mode, which would correspond to a drastic reduction in the neutron dose equivalent received by the patient as contamination of high-energy radiotherapy [37]. In addition, by reducing the radiation time, the possibility of patient movement during the treatment is reduced. As a result, the accuracy of dose delivery to the target volume is improved.

The electron contamination can be generated by the inelastic scattering interactions of high-energy photons with the various components of the LINAC head and the air molecules between the LINAC head and the patient's body surface [15]. These contaminant electrons increase the build-up dose, especially the surface dose. In clinical practice, when designing an optimal treatment plan, this increased surface dose may limit the delivery of the prescribed dose to the target volume depth due to the possibility of an unacceptable absorbed dose by the skin and healthy tissues. From tables 2 and 5, our data for the FF mode shows that applying the 1 Tesla magnetic deflector (MD) removed all electrons from the beam and resulted in 8.3% decrease in the surface dose. Inserting the lead filter decreased the electron fluence by about 64.4% and resulted in 11.2% decrease in the surface dose. Despite more contaminated electrons reaching

the patient's skin when using a lead filter compared to using the magnetic deflector (MD), the surface dose decreases more due to the photon beam absorption and scattering. However, this decrease in photon fluence decreases the dose rate. Consequently, it reduces the delivered dose to tumors in deeper depth, which is a disadvantage of using a lead filter.

The flattening filter exhibits a dualistic role with secondary electrons. It serves as an absorber of secondary electrons generated from the upper components of LINAC's head and prevents them from reaching the patient's body surface; however, it is the primary source of secondary electrons that reach the build-up region [2, 38]. Contaminant electrons significantly contributed to the increasing surface dose by removing the flattening filter [5, 39, 40]. Mesbahi *et al* (2009) reported that removing the flattening filter leads to a notable increase in the fluence of contaminant electrons up to 1.6 times, which has caused increasing radiation dose delivered to the patient's skin [41]. From the data in table 5, the ratio of electron fluence for the FFF mode to the FF mode was 4.18, and removing the flattening filter significantly increased the surface dose from 54.4% to 127.0% (table 2).

Furthermore, the removal of the flattening filter can also result in a change in the energy spectrum of the treatment beam. As shown in tables 4 and 5, the FFF beam tends to have a higher proportion of low-energy photons and electrons (with an average energy of 3.25 MeV and 5.1 MeV, respectively) than the flattened beam (with an average energy of 4.19 MeV and 5.5 MeV, respectively) that is consistent with reported data by Chung *et al* (2016) and Titt *et al* (2006) [33, 42]. Vassiliev *et al* (2006) reported the average energy of 4.50 and 3.24 MeV for the photon beam of the FF and FFF modes, respectively, which are in agreement with our data; however, the estimated data were calculated in a spherical detector located on the central axis beam while our data was determined across the $10 \times 10 \text{ cm}^2$ field size [43]. The reduction of the average energy can be one of the reasons for the shift of the maximum dose depth towards the surface. This altered energy spectrum can have implications for dose calculations and treatment planning. It may require adjustments in treatment planning algorithms and quality assurance procedures to ensure accurate dose delivery and patient safety [36, 44, 45].

Another effect of flattening filter removal is the reduction in beam penumbra; the beam becomes less scattered, resulting in a sharper penumbra calculated from the profile dose at a depth of 10 cm. Our calculated beam penumbra from the dose profile at a depth of 10 cm was 0.77 and 0.69 cm for the FF and FFF mode, respectively, which is in good agreement with the reported data by Spina and Chow (2022) [46]. This can be advantageous in cases where precise dose delivery is crucial, such as in stereotactic radiosurgery or stereotactic body radiation therapy, where the goal is to deliver a high dose to a small target volume while

sparing surrounding healthy tissues [33, 36, 47]; however, the sharper penumbra may increase the sensitivity to patient setup errors and uncertainties in dose calculation algorithms [47]. Additionally, the spread out of the beam was evaluated at the surface depth of the phantom in this study (table 3). The penumbra has increased at the surface depth by removing the flattening filter. This duality (increasing penumbra at surface depth and decreasing penumbra at a depth of 10 cm) can have various causes. The increase of contaminating electrons and decrease of photon's average energy by removing the flattening filter may have caused this penumbra at the surface depth.

4.2. Magnetic deflector (MD) utilization

Magnetic deflectors employ a magnetic field to manipulate charged particles through the Lorentz force, such as contaminant electrons generated in the LINAC head. By deviating contaminant electrons from the beam path and the patient's body, the patient's skin dose can be significantly reduced. Damrongkijudom *et al* (2006) demonstrated that using a magnetic field decreased the number of contaminant electrons reaching the patient's skin, resulting in a 20% reduction in skin dose for $10 \times 10 \text{ cm}^2$ field size of 6 MV photon beam radiotherapy [15]. This study showed that using MD to reduce contamination electrons decreased surface dose in both FF and FFF modes. Compared to the standard mode, this reduction was 8.3% and 16.8% in the FF and FFF modes, respectively. In addition, getting rid of the contaminant electrons, which is the main reason for the maximum dose depth (d_{max}) displacement in FFF mode (3.1 cm), can bring the maximum dose depth back to the maximum dose depth of the FF mode (3.7 cm). Due to more contamination electrons in the FFF mode, removing these contamination electrons by the MD causes a more significant reduction in the penumbra and off-axis dose compared to the FF mode.

4.3. Lead filter utilization

Lead filters are employed in radiation therapy to reduce electron contamination produced in the linear accelerator (LINAC) head [21, 24]. Compton and photoelectric interactions of photons with lead shield due to the high atomic number and density of lead material led to the scattering and absorption of photons, consequently reducing the dose to the patient's skin. Shukla *et al* (2019) reported a 10.4% reduction in surface dose when using a lead filter for a $10 \times 10 \text{ cm}^2$ field size in telecobalt radiation therapy [21]. This study also provides the same that using a lead filter reduced surface dose by 11.2% in FF mode. However, the lead filter also exhibits a dualistic role with secondary electrons. On the one hand, it serves as an absorber of secondary electrons generated from the upper LINAC's head components. On the other hand, the lead filter is responsible for producing secondary

electrons when photons interact with it. These contaminated electrons from the lead filter can reach the patient's body and skin. However, the final result of using a lead filter will be to reduce the electrons reaching the skin. Despite more contaminated electrons reaching the patient's skin when using a lead filter compared to using the magnetic deflector (MD), the surface dose decreases more due to the photon beam absorption and scattering. However, this decrease in radiation photons also leads to a more significant reduction in tumor dose delivery due to a decreased dose rate, which is a disadvantage of using a lead filter to remove the contaminant electrons.

4.4. Magnetic deflector and lead filter utilization

Utilizing a magnetic deflector in conjunction with a lead filter effectively reduces the presence of contaminated electrons, resulting in a significant decrease in surface dose, mainly when operating in the FFF mode. Despite this improvement, certain drawbacks associated with lead filters include reduced photon fluence and dose rate. Consequently, the maximum dose depth (d_{max}) and the dose delivered to deeper regions remain unchanged compared to the scenario where only a lead filter is applied. From our calculated data, simultaneous use of MD and lead filter caused the most decrease in the off-axis dose at a 6 cm distance by 16.45% compared to the FFF mode. Nevertheless, combining a magnetic deflector and lead filter offers notable advantages, including a substantial reduction in un-flatness and penumbra of surface dose profile and off-axis surface dose. These benefits are primarily attributed to the effective removal of contaminant electrons.

5. Conclusion

Our MC model successfully calculated the dosimetric parameters of 18 MV-Varian LINAC with and without a flattening filter, lead shield, and magnetic deflector. Removing the flattening filter increases the dose rate and out-of-field dose. At the same time, removing the flattening filter reduces the dose profile uniformity. Furthermore, the increase in electron contamination causes a decrease in the maximum dose depth and an increase in the skin dose. Using the lead shield at the end of the secondary collimator reduces electron contamination on the phantom surface, but also reduces photon fluence due to attenuation. Our results showed that by using the magnetic deflector (1 T) while removing the contaminating electrons, the increased photon fluence resulting from the removal of the flattening filter is preserved and the maximum dose depth is returned to the depth of the FF mode and the skin protection property is restored. It is not recommended to use the lead shield and the magnetic deflector at the same time, because by applying the

only magnetic field deflector, contaminant electrons are completely removed from the incident beam.

Acknowledgments

This report was a part of the MSc thesis by Morteza Hashemizadeh. This research was funded by the Vice Chancellor for Research Affairs of Ahvaz Jundishapur University of Medical Sciences (Grant No. CRC-0210).

Data availability statement

The data cannot be made publicly available upon publication because no suitable repository exists for hosting data in this field of study. The data that support the findings of this study are available upon reasonable request from the authors.

ORCID iDs

Morteza Hashemizadeh  <https://orcid.org/0009-0000-5499-4563>

Mansour Zabihzadeh  <https://orcid.org/0000-0002-0133-1085>

References

- [1] Parsai E I, Shvydka D, Pearson D, Gopalakrishnan M and Feldmeier J J 2008 Surface and build-up region dose analysis for clinical radiotherapy photon beams *Appl. Radiat. Isot.* **66** 1438–42
- [2] Mesbahi A, Mehnati P and Keshtkar A 2007 A comparative Monte Carlo study on 6MV photon beam characteristics of Varian 21EX and Elekta SL-25 linacs *Int. J. Radiat. Res.* **5** 23–30 (<http://ijrr.com/article-1-290-en.html>)
- [3] Medina A L et al 2004 Comparison between TG-51 and TRS-398: electron contamination effect on photon beam-quality specification *Phys. Med. Biol.* **49** 17–32
- [4] Yani S, Dirgayussa I G E, Rhani M F, Soh R C X, Haryanto F and Arif I 2016 Monte Carlo study on electron contamination and output factors of small field dosimetry in 6 MV photon beam *Smart Science* **4** 87–94
- [5] Haryanto F, Rhani M F, Anam C and Yani S 2022 Investigation of electron contamination on flattened and unflattened varian clinac iX 6X and 15X photon beam based on monte carlo simulation *Atom Indonesia* **48** 147–58
- [6] Tsiamas P et al 2014 Beam quality and dose perturbation of 6 MV flattening-filter-free linac *Physica Med.* **30** 47–56
- [7] Chung J et al 2015 Comparison of VMAT-SABR treatment plans with flattening filter (FF) and flattening filter-free (FFF) beam for localized prostate cancer *J. Appl. Clin. Med. Phys.* **16** 302–13
- [8] Ashokkumar S et al 2015 Measurement and comparison of head scatter factor for 7 MV unflattened (FFF) and 6 MV flattened photon beam using indigenously designed columnar mini phantom *Reports of Practical Oncology & Radiotherapy* **20** 170–80
- [9] Wang Y, Khan M K, Ting J Y and Easterling S B 2012 Surface dose investigation of the flattening filter-free photon beams *International Journal of Radiation Oncology* Biology* Physics* **83** e281–5
- [10] Najem M A, Spyrou N M, Podolyák Z and Abolaban F A 2014 The physical characteristics of the 15MV Varian Clinac 2100C unflattened beam *Radiat. Phys. Chem.* **95** 205–9
- [11] Kry S F et al 2007 Reduced neutron production through use of a flattening-filter-free accelerator *International Journal of Radiation Oncology* Biology* Physics* **68** 1260–4
- [12] Pichandi A, Ganesh K M, Jerin A, Balaji K and Kilara G 2014 Analysis of physical parameters and determination of inflection point for flattening filter Free beams in medical linear accelerator *Reports of Practical Oncology & Radiotherapy* **19** 322–31
- [13] Harper N R, Metcalfe P E, Hoban P W and Round W H 1991 Electron contamination in 4 MV and 10 MV radiotherapy x-ray beams *Australasian Physical & Engineering Sciences in Medicine* **14** 141–5 Available from <http://europepmc.org/abstract/MED/1953499>
- [14] Malataras G, Kappas C and Lovelock D M J 2001 A Monte Carlo approach to electron contamination sources in the Saturne-25 and -41 *Phys. Med. Biol.* **46** 2435–46
- [15] Damrongkijudom N, Oborn B, Butson M and Rosenfeld A 2006 Measurement of magnetic fields produced by a ‘Magnetic deflector’ for the removal of electron contamination in radiotherapy *Australasian Physical & Engineering Sciences in Medicine* **29** 321–7
- [16] Zhu T C and Palta J R 1998 Electron contamination in 8 and 18 MV photon beams *Med. Phys.* **25** 12–9
- [17] Sjögren R and Karlsson M 1996 Electron contamination in clinical high energy photon beams *Med. Phys.* **23** 1873–81
- [18] Yorke E D, Ling C C and Rustgi S 1985 Air-generated electron contamination of 4 and 10 MV photon beams: a comparison of theory and experiment *Phys. Med. Biol.* **30** 1305–14
- [19] Oborn B M, Kolling S, Metcalfe P E, Crozier S, Litzberg D W and Keall P J 2014 Electron contamination modeling and reduction in a 1 T open bore inline MRI-linac system *Med. Phys.* **41** 051708
- [20] Rogers D W O 1999 Correcting for electron contamination at dose maximum in photon beams *Med. Phys.* **26** 533–7
- [21] Shukla R, Patel N P, Yadav H P and Kaushal V 2019 A Monte Carlo simulation study on the effectiveness of electron filters designed for telecobalt radiation therapy treatment *International Journal of Radiation Research* **17** 217–27
- [22] Moumennezhad M, Bahreyni Toosi M, Sadeghi R, Gholam H H and Naseri S H 2010 A Monte Carlo simulation and dosimetric verification of physical wedges used in radiation therapy *Int. J. Radiat. Res.* **7** 223–7 (<http://ijrr.com/article-1-583-en.html>)
- [23] Lye J E et al 2016 Comparison between the TRS-398 code of practice and the TG-51 dosimetry protocol for flattening filter free beams *Phys. Med. Biol.* **61** N362–72
- [24] Li X A and Rogers D W O 1994 Reducing electron contamination for photon beam-quality specification *Med. Phys.* **21** 791–7
- [25] Andersson F, Barberet P, Incerti S and Moretto P 2008 A detailed ray-tracing simulation of the high resolution microbeam at the AIFIRA facility *Nucl. Instrum. Methods Phys. Res. B* **266** 1653–8
- [26] Incerti S et al 2007 Monte Carlo simulation of the CENBG microbeam and nanobeam lines with the Geant4 toolkit *Nucl. Instrum. Methods Phys. Res. B* **260** 20–7
- [27] Incerti S, Habchi C, Moretto P, Olivier J and Seznec H 2006 Geant4 simulation of the new CENBG micro and nanoprobe facility *Nucl. Instrum. Methods Phys. Res. B* **249** 738–42
- [28] Incerti S et al 2005 A comparison of ray-tracing software for the design of quadrupole microbeam systems *Nucl. Instrum. Methods Phys. Res. B* **231** 76–85
- [29] Bull J 2011 *Magnetic Field Tracking Features in MCNP6* LA-UR-11-00872 (Los Alamos National Laboratory)
- [30] Goorley T et al 2012 Initial MCNP6 release overview *Nucl. Technol.* **180** 298–315
- [31] Goorley T 2014 MCNP6. 1.1-beta release notes. LA-UR-14-24680
- [32] Das S, Kharade V, Pandey V P, Kv A, Pasricha R K and Gupta M 2022 Gamma index analysis as a patient-specific quality assurance tool for high-precision radiotherapy: a clinical perspective of single institute experience *Cureus.* **14** e30885

- [33] Chung J B, Kang S W, Eom K Y, Song C, Choi K S and Suh T S 2016 Comparison of dosimetric performance among commercial quality assurance systems for verifying pretreatment plans of stereotactic body radiotherapy using flattening-filter-free beams *J. Korean Med. Sci.* **31** 1742
- [34] Vassiliev O N, Kry S F, Chang J Y, Balter P A, Titt U and Mohan R 2009 Stereotactic radiotherapy for lung cancer using a flattening filter free Clinac *J. Appl. Clin. Med. Phys.* **10** 14–21
- [35] Baic B, Kozłowska B, Kwiatkowski R and Dybek M 2019 Clinical advantages of using unflattened 6-MV and 10-MV photon beams generated by the medical accelerator Elekta Versa HD based on their dosimetric parameters in comparison to conventional beams *Nukleonika* **64** 77–86
- [36] King R B et al 2013 An *in vitro* study of the radiobiological effects of flattening filter free radiotherapy treatments *Phys. Med. Biol.* **58** N83–94 Available from: <https://iopscience.iop.org/article/10.1088/0031-9155/58/5/N83>
- [37] Kry S F et al 2007 Reduced neutron production through use of a flattening-filter-free accelerator *Int. J. Radiat. Oncol. Biol. Phys.* **68** 1260–4
- [38] Ulmer W, Pyry J and Kaissl W 2005 A 3D photon superposition/convolution algorithm and its foundation on results of Monte Carlo calculations* *Phys. Med. Biol.* **50** 1767–90
- [39] Maulana I F, Yani S, Sumaryada T, Rhani M F and Haryanto F 2023 Commissioning of Elekta Infinity™ 6 MV flattening filter-free using Monte Carlo simulation. *Radiat. Phys. Chem.* **210**
- [40] Vagena E, Stoulos S and Manolopoulou M 2016 Geant4 simulations on medical Linac operation at 18MV: Experimental validation based on activation foils *Radiat. Phys. Chem.* **120** 89–97
- [41] Mesbahi A 2009 A Monte Carlo study on neutron and electron contamination of an unflattened 18-MV photon beam *Appl. Radiat. Isot.* **67** 55–60
- [42] Titt U, Vassiliev O N, Pönisch F, Dong L, Liu H and Mohan R 2006 A flattening filter free photon treatment concept evaluation with Monte Carlo *Med. Phys.* **33** 1595–602
- [43] Vassiliev O N, Titt U, Pönisch F, Kry S F, Mohan R and Gillin M T 2006 Dosimetric properties of photon beams from a flattening filter free clinical accelerator *Phys. Med. Biol.* **51** 1907–17
- [44] Adamczyk M, Kruszyna-Mochalska M, Rucińska A and Piotrowski T 2020 Software simulation of tumour motion dose effects during flattened and unflattened ITV-based VMAT lung SBRT *Reports of Practical Oncology & Radiotherapy* **25** 684–91
- [45] Mamballikalam G, Senthilkumar S, Clinto C O, Ahamed Basith P M, Jaon Bos R C and Thomas T 2021 Time motion study to evaluate the impact of flattening filter free beam on overall treatment time for frameless intracranial radiosurgery using Varian TrueBeam® linear accelerator *Rep. Pract. Oncol. Radiother.* **26** 111–8
- [46] Spina A and Chow J C L 2022 Dosimetric impact on the flattening filter and addition of gold nanoparticles in radiotherapy: a Monte Carlo study on depth dose using the 6 and 10 MV FFF photon beams *Materials* **15** 7194
- [47] Vassiliev O, Kry S, Chang J, Balter P, Titt U and Mohan R 2007 SU-FF-T-387: stereotactic radiotherapy for lung cancer using flattening filter free accelerator *Med. Phys.* **34** 2491